



Shear plane characteristics of geocell-reinforced fine sand through direct shear test

Hao Li¹ · Xiaohua Yang¹ · Hao Zeng¹ · Xu Zhao¹

Received: 15 December 2020 / Accepted: 13 October 2021 / Published online: 28 October 2021
© Saudi Society for Geosciences 2021

Abstract

Although geocells are widely used, most current research focuses on improving the bearing capacity of foundations. Only few studies have investigated the shear strength of soil reinforced by geocells, especially the shear plane characteristics, which are important design consideration. A series of large-scale direct shear tests was conducted on fine sand to investigate the shear plane behavior influenced by different parameters including cell size (509.6 cm² and 2041.8 cm²), geocell angle of inclination to the horizontal plane (0° and 45° + $\varphi/2$), and normal stress (100 kPa, 200 kPa, 300 kPa, and 400 kPa) on the sample in reinforced and unreinforced soil. To study the shear strength of the shear plane in unreinforced and geocell-reinforced conditions, shear characteristics mobilized at the shear plane including apparent cohesion, friction angle, and dilation were evaluated. The results revealed that smaller cells produce a better reinforcement effect; the geocell angle of inclination to the horizontal plane has an effect on the shape of the shear displacement versus shear stress curve. An angle of 0° produces a strain-softening curve, and the curve with a geocell angle of 45° + $\varphi/2$ produces shear stress that continues to increase with displacement. It has been reported that increasing normal stress weakens the ability of geocells to reinforce soil under both maximum shear stress conditions and the residual conditions. Contraction was observed at the beginning of the test, the dilation gradually decreased with an increase in normal stress. The main factor influencing the dilation is geocells' angle of inclination to the horizontal plane; the cell size has little effect on the dilatancy of the samples.

Keywords Geocell · Fine sand · Direct shear test · Interface · Shear strength · Dilation

Introduction

In recent years, geocell applications have grown rapidly owing to their cost-effectiveness, environmental friendliness, durability, and ease of use (Hegde 2017). Geocells are often used to strengthen a foundation and increase the bearing capacity of footings (Thallak et al. 2007; Zhou and

Wen 2008; Madhavi Latha and Somwanshi 2009; Chen et al. 2013a,b; Hegde and Sitharam 2013; Neto et al. 2013; Moghaddas Tafreshi et al. 2015; Biabani et al. 2016; Abdulmuttalip and Gizem 2021). It has been demonstrated that geocells are an ideal material for significantly improving the bearing capacity of a foundation and reducing settlement; the effects of geocell geometry, foundation bed properties, and soil materials have also been studied. Dash Sujit (2010, 2012) reported the influence of relative soil density and geocell type on the performance improvement with geocell reinforcement, indicating that a high relative density and a smaller geocell produce a better reinforcement effect. Tavakoli Mehrjardi et al. (2019) studied the scale effect on the behavior of geocell-reinforced soil. It was recommended that the cell size, particle size, and foundation width are proportional to each other to obtain the best reinforcement effect.

In addition to foundation reinforcement, geocells are also used to strengthen slopes and build retaining structures (Yang 2005). In retaining walls, geocell reinforcements are mainly subjected to lateral earth pressure, and the shear

Responsible Editor: Zeynal Abiddin Erguler

✉ Xiaohua Yang
xiaohuay@chd.edu.cn

Hao Li
2018021005@chd.edu.cn

Hao Zeng
674286358@qq.com

Xu Zhao
2018221048@chd.edu.cn

¹ School of Highway, Chang'an University, Xi'an 710064, China

resistance of the soil reinforced by geocells is particularly critical. Chen et al. (2013b) presented a numerical analysis of the behavior of geocell-reinforced retaining structures with different layouts. It was found that extending the length of geocells in some layers to serve as reinforcement reduced the deformation of the structure and decreased the potential slip zone. Song et al. (2018) conducted numerical analyses on the failure mode of geocell-reinforced retaining walls; the results indicated that the failure surface will cut through the retaining wall and finally develop to the wall toe when friction angle $\geq 20^\circ$. Khorsandiardabili and Ghazavi (2021) proposed an analytical approach to investigate the stability of geocell-reinforced slopes; this approach considered each geocell layer as a beam providing bending and shear resistance in addition to axial strength to optimize the lengthy reinforcement system.

Researchers tend to use triaxial tests to explore the shear strength of geocell composites. Bathurst and Karpurapu (1993) revealed that the stiffening effect and strength increase imparted to the soil through enhanced confinement and a simple elastic membrane model can be used to estimate the additional apparent cohesion present in the composite structure. Chen (2013) found that cell size is the most significant factor affecting the apparent cohesion; and circular cells induce the highest apparent cohesion. Rajagopal et al. (1999) investigated the effect of geocell stiffness on the overall performance of a geocell–soil composite using fabricated geocells. Zhang et al. (2006) reported that 3-D reinforcement increases both apparent cohesion and the angle of internal friction in the soil. Besides triaxial tests, direct shear tests are widely used to investigate the shear plane's strength. But research on the interface characteristics of soil and geosynthetics focuses mainly on geogrids (Liu et al. 2009; Lopes and Silvano 2010; Ferreira et al. 2015; Hatami and Esmaili 2015). Yang (2005) chose loess and sand as soils to study the strength of reinforced soil, with the geocell–soil composite sheared in the horizontal and 45° to the horizontal plane. Wang et al. (2008) found that the unreinforced soil and geocell-reinforced soil give similar nonlinear features on the behavior of shear stress and displacement. Tavakoli Mehrjardi and Motarjemi (2018) reported that the shear strength at the geocell–soil interface was increased by increasing the median grain size and relative density of the soil. Arvin et al (2021) conducted large-scale shear test on the geocell–geofoam composite samples and found that inclusion of the geocell leads to a considerable increase in the shear strength and a great decline in the compressibility of the geofoam. Simoni and Houlsby (2006) reported that the presence of coarse particles can improve the shear strength and dilatancy through direct shear tests on the sand–gravel mixture. Ferreira et al. (2015) found that the vertical contraction of the looser soil tended to increase with applied normal stress and soil moisture content. In direct

shear tests with denser soil samples, the soil dilation tended to increase with decreasing normal stress and moisture content. Afzali Nejad et al. (2018) confirmed that both the peak and maximum dilation angles of sand–geosynthetic interfaces are affected by soil inherent anisotropy.

The stress applied on the shear plane is very complicated; to study the characteristics of the geocell-reinforced shear plane, the angle of 0° and $45^\circ + \varphi/2$ inclined geocell was introduced in this study, where φ represents the friction angle of the soil, and it can be obtained through a direct shear test on unreinforced soil. This study investigates the effect of geocell properties on the shear strength of the plane and estimates the effectiveness of geocell reinforcement; the dilatancy of the geocell-reinforced sand was considered as well. It is meaningful for the study of the characteristics of shear plane and also has reference value in the application of geocell-reinforced earth retaining walls.

Test materials

In this study, fine sand and geocells with different dimensions were used as test materials, and a pair of large-scale shear boxes was created for the direct shear tests. Automatic hydraulic system was the source of horizontal force applied on the shear boxes. The vertical force is provided by the reaction frame and a jack. In addition, many other devices such as pressure sensor and dial indicators are also necessary.

Geocells

A geocell is a type of honeycomb structure constructed of heat-bonded nonwoven (HBNW) strips. Two strips were connected by seams to form a three-dimensional grid, and two types of geocells were used in this study. The distance between the seams of each cell was 400 mm and 800 mm, resulting in the cells with an area of 509.6 cm² and 2041.8 cm², respectively. The thickness and height of the cell are customized according to different application requirements, and the cell thickness and height in this paper are 1.75 mm and 20 cm. The physical properties can get from manufactures, but the parameters related to raw materials such as tensile strength must be obtained through experiments. The characteristics of the cell are greatly affected by the strip material, and the cause of cell failure is stretching; to investigate the ultimate tensile strength of the strip, a tensile test of strip was carried out according to Test Methods of Geosynthetics for Highway Engineering (JTGE50-2006). It was found that the ultimate tensile strength of the strip is 14.2kN/m, which illustrated that the cell has a high tensile strength and can withstand great tensile stress. The surface of the geocell is textured, and it can increase the friction

with the soil. Table 1 summarizes the properties of the geocells used in this study.

Large-scale shear box

To study the characteristics of the shear plane, a pair of shear boxes including a lower box and an upper box was constructed for the large-scale shear test. The box material is a steel plane with a thickness of 20 mm and a height of 200 mm, and the steel plates are connected by bolts to form a frame. The shear box is a square with a side length of 40 cm. During the test, the upper box was fixed, and a horizontal force was applied to the lower box to achieve shearing. The soil sample was covered with a steel plate to transmit the vertical pressure exerted by the jack and the reaction frame. Actually, large-scale shear box has an impact on the shear strength, and the normal force in the shear plane is induced not only the exerting force but also the weight of the upper box with soil and the rolling friction force at the fixed end of the upper box.

Table.1 Technical indicators of geocells

Properties	Unit	Value
Density	g/cm ³	0.96
Cell area	cm ²	509.6 and 2041.8
Cell height	mm	200
Cell thickness	mm	1.75
Ultimate tensile strength	kN/m	14.2

Cell area refers to the area of the equivalent circle for each cell

To avoid friction, a gap between the upper box and the lower box was created (Fig. 2a and b), and the lubricant was applied between the boxes to reduce friction. Both the lower box and the bottom plates were equipped with tracks, and two rows of steel balls were placed in the tracks. However, there still be rolling friction; the measured horizontal force is the sum of the shear force in the shear plane but also the rolling friction between the box and the tracks. Besides, the force systems generate a moment in the shear plane. Although the large shear box can meet the requirements for investigating the shear strength of the soil reinforced by geocells, the error caused by the apparatus should be considered. To evaluate the impact of the large shear box on the test, the inherent resistance of the device was measured to calibrate the large-scale direct shear apparatus; in addition, a series of standard direct shear tests on fine sand was carried out as control group.

Soil

The soil is SP-SM (poorly graded sand with silt) as per Unified Soil Classification System; its particle grading curve was obtained through a sieve test, as shown in Fig. 1a. The grain size results indicate that 92.2% of the particles were between 0.425 mm and 0.075 mm in size and 7.8% of the particles were smaller than 0.075 mm, including silt of 6.7% and clay of 1.1%.

It was determined through a compaction test that the maximum dry density of the soil was 1.635 g/cm³ and the optimum water content was 9.5%. Figure 1b shows the compaction curve of the soil, which is different from that of the cohesive soil. The curve has two peak points, corresponding

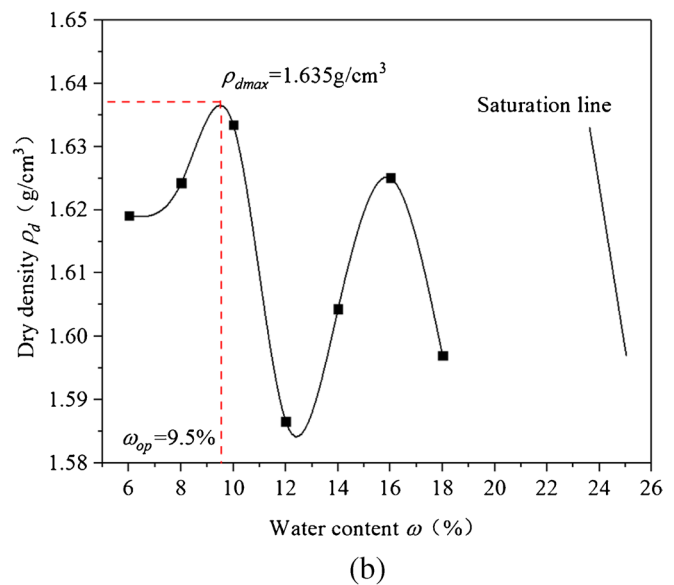
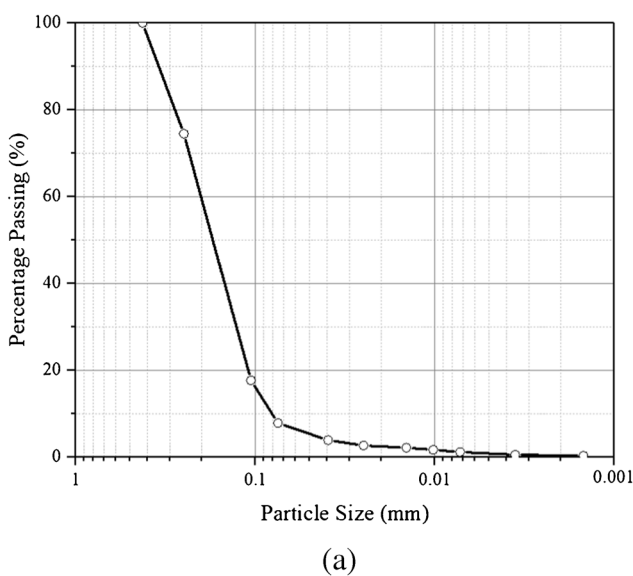


Fig. 1 a Particle grading curve of the soil. b Compaction curve of the soil

Table.2 Properties of the soil

Properties	Value
Specific Gravity (G_s)	2.66
Wet density (ρ)	1.87 g/cm ³
Maximum dry density (ρ_{dmax})	1.64 g/cm ³
Optimum water content (ω_{op})	9.5%
Void ratio (e)	0.68

Table.3 Test program

Test no	Soil	Sample	Cell area (cm ²)	Angle
1	Sand	S	—	0°
2	Reinforced sand	RS400	509.6	0°
3	Reinforced sand	RS800	2041.8	0°
4	Reinforced sand	RS400*	509.6	45° + $\varphi/2$
5	Reinforced sand	RS800*	2041.8	45° + $\varphi/2$

1. S sand, R reinforced

2. “400” indicates the distance between two seams of the cell was 400 mm; “800” indicates that this distance was 800 mm. An angle of 45° + $\varphi/2$ to the horizontal plane is indicated by “*”; otherwise, the angle is 0°

to water contents of 9.5% and 16.5%. During the test, the dry density gradually increased with the water content, then reaching the first peak, and as the water content further increased, the dry density reached the second peak point and then drops down. The properties of the soil are presented in Table 2.

Test program

Five experimental groups were designed according to reinforcement, cell area, and the geocell angle of inclination to the horizontal plane (Table 3). Test 1 was unreinforced; the other tests used geocells reinforcement with different cell areas and geocell angles in the apparatus.

The soil should be compacted under the optimal water content condition. The weight of soil was calculated based on the volume of the box V , the compaction degree, the maximum dry density ρ_{dmax} , and the optimum water content ω_{op} . When preparing the soil samples, the geocell was paved in the lower box firstly. Then the soil was poured into the mold in several layers of about 5 cm thickness. Layers were compacted by a light hammer. The upper box was placed over the lower box, and the operation was repeated until the upper box was filled. To simulate the subgrade retaining wall, the compaction degree in the test is 93%.

Before the shear test with a 45° + $\varphi/2$ inclined geocell (φ is friction angle of the soil), the position of geocell in the apparatus should be determined. Firstly, draw a 45° + $\varphi/2$

line on the shear box, then infill the box and compact it following the line, and pave the geocell on the soil wedge. To compact the soil in the geocell, a light hammer was used, with a cylindrical head of steel; this hammer head can detach from its body and fit the size of each cell. The soil in the boxes should be compacted according to the compaction degree. Two schematic views of the direct shear apparatus are shown as Fig. 2a and Fig. 2b, the arrangement of 0° and 45° + $\varphi/2$ cell layer in the test is shown as Fig. 2c and Fig. 2d.

A horizontal servo loading system was used in the tests; the normal force was provided by the reaction frame and a jack and was measured by a pressure sensor between the frame and the jack. The value of normal force exerted on the box cap is shown in Table 4.

During the test, the shear speed was 0.8 mm/min until failure. There are usually two criteria for the failure value. If the shear–stress displacement curve had a significant peak or a stable value, this value was used as the shear strength value. If the shear stress increased with shear displacement and there was no peak or stable value, the shear stress corresponding to a selected shear displacement was used as the shear strength value. Generally, the maximum shear displacement is 1/15–1/10 of the sample diameter, accordingly; the termination condition for this test is that the shear force is reduced or the shear displacement reaches 40 mm. During the shearing, all data including the displacement of the box, the shear force, the normal force, and dilation were recorded.

Prior to shearing, normal stress was applied to the samples for 1 h to stabilize the particles from any possible creep. During the test, the horizontal displacement and force were measured by the servo loading system and recorded through the host computer; vertical displacement was measured by dial indicators. Many of the tests were repeated three times to check the consistency of the results.

Results and discussion

Figure 3 presents the shear–stress and shear displacement curves for all five experimental conditions under normal stresses of 100 kPa (Fig 3a), 200 kPa (Fig 3b), 300 kPa (Fig 3c), and 400 kPa (Fig 3d). Test 1, represented by the letter “S,” used the fine sand soil without geocells; the shear stress of the shear plane was obviously smaller than in other tests (Table 5), indicating that the presence of geocells significantly improved the shear strength of the soil regardless of the normal stress.

In the initial stages of the test, all shear stresses increased rapidly before the curve stabilized; however, their stabilization paths were different. For the first three test conditions (S, RS400, RS800), with an geocell angle of 0° to the horizontal plane, the displacement–stress curves exhibited a peak point, indicating that the maximum shear

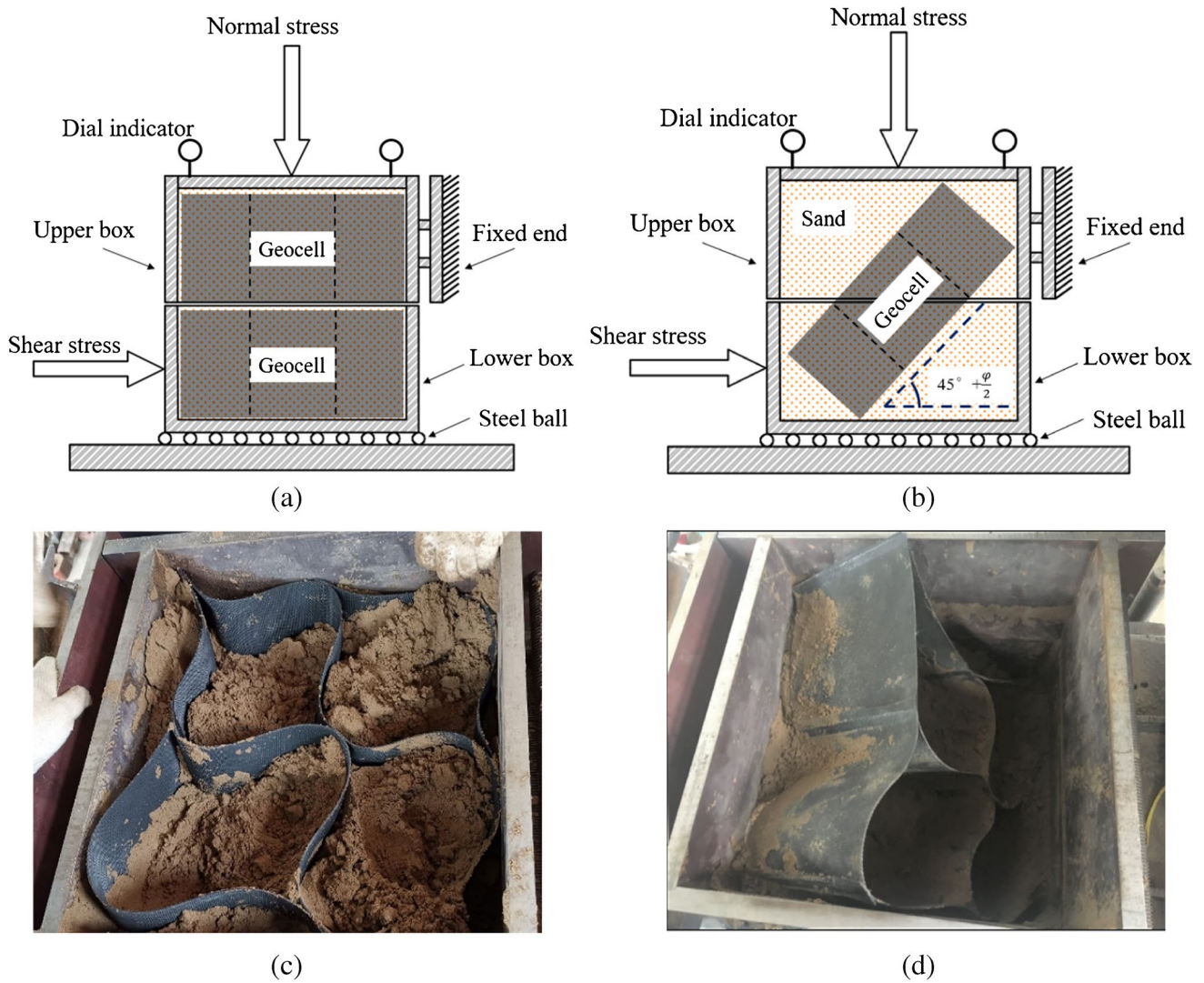


Fig. 2 Schematic view of direct shear apparatus

Table.4 Normal force acting on box’s cap

Box area (mm ²)	Normal force (kN)			
	100 kPa	200 kPa	300 kPa	400 kPa
400 × 400	16	32	48	64

stress decreased to a specific residual shear strength. However, test 4 (RS400*) and test 5 (RS800*) did not show this phenomenon; as the shear displacement increased, their curves continued to increase without yielding, but the growth rate slowed. When the angle is $45^\circ + \varphi/2$ to the horizontal plane, the shear plane can withstand greater shear stress. This implies that geocell improves the shear strength of the hybrid plane, because the shear plane consists of soil and geocell, and the geocell provides a great tensile strength. In addition, the shear displacement

corresponding to the peak point increased with an increase in the normal stress. In other words, under heavy normal stress, the appearance of the peak point is delayed.

To evaluate the ability of geocells to reinforce fine sand, the ratio of the shear strength of reinforced soil $(\tau_{max})_R$ to the shear strength of unreinforced soil $(\tau_{max})_{Soil}$ is defined as an influencing factor. In Table 6, the value $(\tau_{max})_R / (\tau_{max})_{Soil}$ varies between 1.09 and 1.36; a value greater than 1.0 indicates that the geocell enhances the shear plane irrespective of cell area and angle conditions. However, by comparing different cell sizes, it was found that although small cells can provide better reinforcement, the difference is small; the use of larger geocells may provide better economic benefits. An increase in normal stress hinders the positive effect of geocell reinforcement on the shear plane; that is, the reinforcement effect of the geocell is more obvious when the vertical stress is lower.

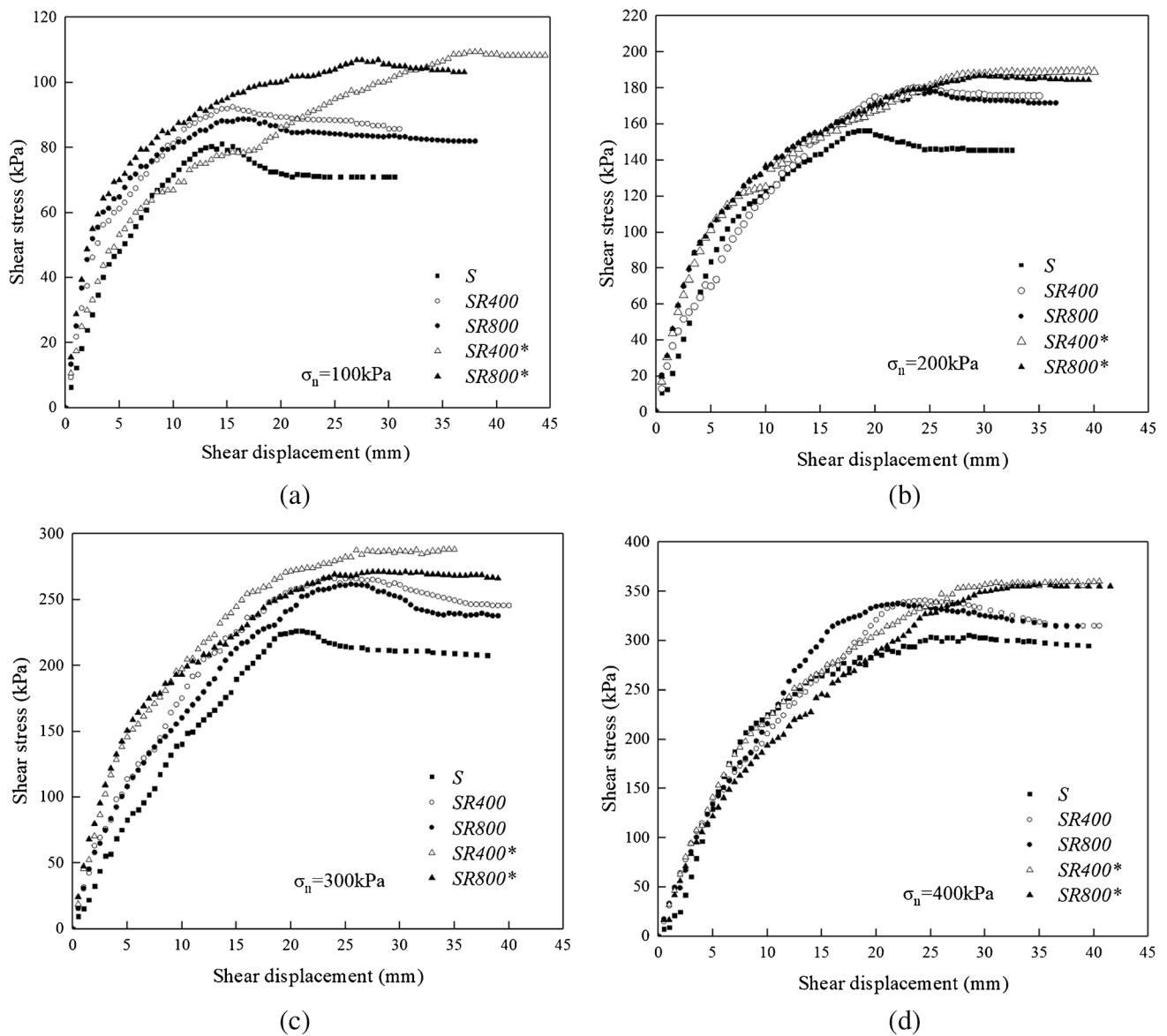


Fig. 3 Shear stress versus shear displacement of direct shear test under different normal stresses

Maximum apparent cohesion

By comparing the results obtained from the standard direct shear test (represented by S_0) and the large-scale direct shear test, it can be found that the cohesion and friction angle obtained by large-scale shear test are greater, especially cohesion. It is inferred that due to the larger model, the rolling friction between the lower box and the tracks and the soil weight in upper box were magnified, and the loading systems including horizontal and vertical loading system could generate a moment on the sample, resulting in unreinforced sand exhibits false cohesion.

To study the shear strength of the reinforced soil, the linear Mohr failure envelopes under maximum and residual

conditions were exhibit in Fig. 4. It can be found that the envelopes of $RS400$ and $RS400^*$ are above $RS800$ and $RS800^*$, indicating that smaller cells produce better reinforcement effects because their tightening rate is greater than that of larger cells.

For reinforced soil, the intercept between the failure envelope and the y-axis is considered the apparent cohesion. It was observed that geocells greatly strengthened the apparent cohesion of the soil. The analysis is as follows.

The effect of cell size on apparent cohesion is expressed as increasing apparent cohesion with decreasing cell size. The apparent cohesion of sample S is 5.94 kPa; $RS400$ and $RS800$ are 11.25 kPa and 9.58 kPa, 1.9 times and 1.6 times greater than for S , representing an increase of 89.4% and

Table.5 Results of maximum shear stress under different normal stresses

Test no	Sample	Maximum shear stress (τ_{max}) (kPa)				
		$\sigma_n = 100$ kPa	$\sigma_n = 200$ kPa	$\sigma_n = 300$ kPa	$\sigma_n = 400$ kPa	
1	S	81.21	157.67	226.25	303.75	
2	RS400	91.25	180.02	266.13	340.79	
3	RS800	88.75	178.13	261.37	337.25	
4	RS400*	110.63	188.65	287.22	360.00	
5	RS800*	106.88	186.88	271.75	356.08	

Table.6 Values of influence factor under maximum shear stress condition

Sample	$(\tau_{max})_R / (\tau_{max})_{Soil}$			
	$\sigma_n = 100$ kPa	$\sigma_n = 200$ kPa	$\sigma_n = 300$ kPa	$\sigma_n = 400$ kPa
RS400	1.12	1.14	1.18	1.12
RS800	1.09	1.13	1.16	1.11
RS400*	1.36	1.20	1.27	1.19
RS800*	1.32	1.19	1.20	1.17

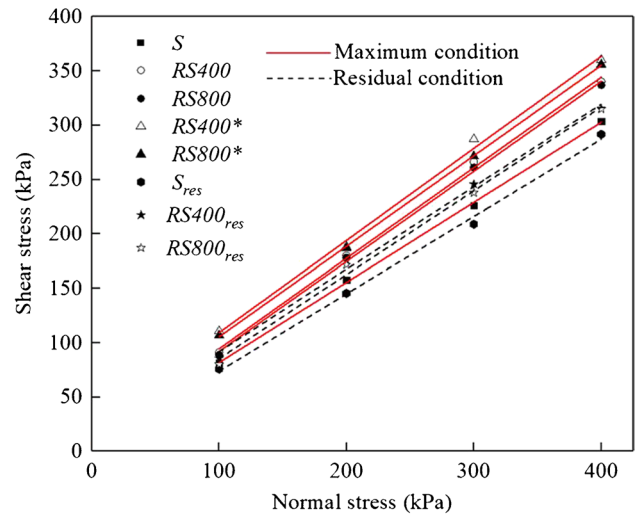


Fig. 4 Linear Mohr failure envelopes under maximum and residual conditions

61.3%, respectively. When the angle that inclination to the horizontal plane is $45^\circ + \varphi/2$, the increase is even greater, reaching 315.7% (RS400*) and 268.4% (RS800*). The influence of the angle of inclination to the horizontal plane on apparent cohesion is greater than the influence of cell size. For comparison, the apparent cohesion of RS400* is approximately 2.2 times that of RS400 and 4.2 times that of S. The reason is that the geocell wraps soil to form a hybrid plane, and the strength of the shear plane is a combination of the geocell and soil resistance to the applied stress (Table 7).

Maximum friction angle

The angle between the Mohr failure envelope and the horizontal axis represents the internal friction angle of the soil. Through experiments, it was found that the geocell can increase the friction angle of the fine sand, but the improvement is limited.

Table 8 summarizes the interface friction angle for all five sample types. In the horizontal shear test, the friction angles of RS400 and RS800 increased by 3.18° and 3° , representing an increase of 8.7% and 8.2%, respectively. In the inclined

Table.7 Interface’s apparent cohesion for all 5 types sample

Test no	Sample	Apparent cohesion (kPa)	Increased value (kPa)	Increased ratio
1	<i>S₀</i>	1.52	—	—
2	<i>S</i>	5.94	—	—
3	<i>RS400</i>	11.25	5.31	89.4%
4	<i>RS800</i>	9.58	3.64	61.3%
5	<i>RS400*</i>	24.69	18.75	315.7%
6	<i>RS800*</i>	21.88	15.94	268.4%

Table.8 Interface’s friction angle for all 5 types sample

Test no	Sample	Friction angle (°)	Increased value (°)	Increased ratio
1	<i>S₀</i>	36.10	—	—
2	<i>S</i>	36.66	—	—
3	<i>RS400</i>	39.84	3.18	8.7%
4	<i>RS800</i>	39.66	3	8.2%
5	<i>RS400*</i>	40.28	3.62	9.9%
6	<i>RS800*</i>	39.93	3.27	8.9%

shear test with an angle of $45^\circ + \phi/2$, *RS400** and *RS800** increased by 3.62° and 3.27° , representing an increase of 9.9% and 8.9%, respectively. The effect of geocells on the friction angle of fine sand is less significant than the effect on apparent cohesion.

Generally, confinement by the geocell increased the apparent cohesive strength of the fine sand; an increase in the internal friction angle had little effect on the shear strength.

Residual shear strength

For the residual shear strength of the samples, this study only examined the first three test conditions (*S*, *RS400*, *RS800*) because there were peak points on their shear–stress displacement curves. Table 9 presents the residual shear stress of each sample under different normal stresses. It is obvious that the residual shear strength increases with an increase in normal stress with or without geocell reinforcement. As with the maximum shear strength, the residual strength of soil with geocell reinforcement is greater than that of unreinforced soil; *RS400* demonstrated the greatest residual strength.

Figure 4 also shows the residual shear strength envelopes for the first three test conditions. The residual friction angle and apparent cohesion values are presented in Table 10. Compared with the maximum strength parameters, the friction angle and the apparent cohesion are reduced by

Table.9 Residual shear strength

Test no	Sample	Residual shear stress τ_{res} (kPa)			
		$\sigma_n = 100$ kPa	$\sigma_n = 200$ kPa	$\sigma_n = 300$ kPa	$\sigma_n = 400$ kPa
1	<i>S</i>	75.86	145.51	208.90	291.63
2	<i>RS400</i>	85.75	175.63	245.78	315.10
3	<i>RS800</i>	80.02	171.75	237.88	314.90

Table.10 Interface’s residual shear strength parameters

Test no	Sample	Friction angle φ_{res} (°)	Apparent cohesion c_{res} (kPa)
1	S	35.4	2.8
2	RS400	37.6	8.4
3	RS800	37.2	16.0

1.3°–2.5° and 2.85–6.42 kPa, respectively. The decrease in the residual friction angle is small, which is mainly reflected in a decrease in the apparent cohesion. Geocell reinforcement mainly affects the apparent cohesion.

To assess the geocell reinforcement capability in improving the shear characteristics of the interface under residual conditions, the influence factor $(\tau_{res})_R/(\tau_{res})_{Soil}$ was studied in this section (Table 11). As with the results for maximum shear stress, the geocell can provide additional reinforcement, but the values are slightly smaller than $(\tau_{max})_R/(\tau_{max})_{Soil}$, indicating that the reinforcement effect becomes weaker, and excessive normal stress reduces the effect. Under heavy normal stress, the internal stress in the soil–geocell composite is increased when subjected to shearing. Although the geocell has better ductility and the surface may not be damaged, the geocell seam may not be able to withstand such pressure.

Dilation

It is known that the volume of sand changes when subjected to shearing. Normally, low-density sand shrinks and medium-density sand undergoes dilation. However, geocells were not considered in previous studies. Due to a lack of relevant specifications for geocells/geosynthetics, there are few studies on the interface between two layers of geocell-reinforced soil. This paper investigated the strength of the shear plane and also the change in the sample volume, that is, the vertical displacement during the shearing process.

To better understand the volume change in samples reinforced by geocells, the dilation of samples under different normal stresses was studied. Figure 5 plots dilation versus shear displacement for all tests under normal stresses of 100–400 kPa. At the beginning of the test, the geocell-reinforced and unreinforced soils both undergo a

Table.11 Values of influence factor under residual condition

Sample	$(\tau_{res})_R/(\tau_{res})_{Soil}$			
	$\sigma_n = 100$ kPa	$\sigma_n = 200$ kPa	$\sigma_n = 300$ kPa	$\sigma_n = 400$ kPa
RS400	1.13	1.20	1.17	1.08
RS800	1.05	1.18	1.13	1.07

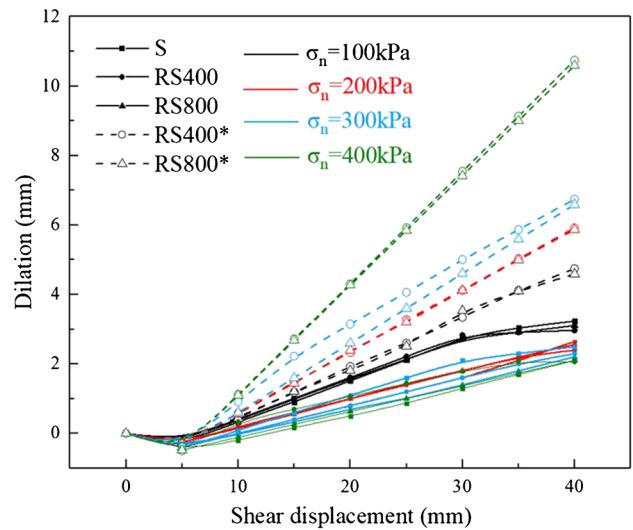


Fig. 5 Dilation versus shear displacement of direct shear test under different normal stresses

vertical contraction as the shear displacement is small; the contraction is proportional to the normal stress. Due to the confinement effect of the geocell on the soil, the contraction of the geocell-reinforced soil is smaller than that of the unreinforced soil; the samples exhibit dilatancy with an increase in shear displacement. When the normal stress is smaller, the samples exhibit stronger dilatancy and greater vertical displacement. When the angle is $45^\circ + \varphi/2$ to the horizontal plane, the dilatancy displacement is significantly greater than that of the angle of 0° ; when the angles are the same, the size of the cell has little effect on the vertical displacement.

This can be interpreted as follows: when the geocell is $45^\circ + \varphi/2$ inclined in the shear box, the shear plane consists of soil and geocell, which causes a heterogeneous compression modulus. When the sample is subjected to vertical loads, the reinforcement soil shrinks unevenly, resulting in the two boxes moving to form a gap that increases vertical displacement, especially under heavy normal stress. Figure 6 shows the gap that the RS800* sample was sheared under 400 kPa normal stress.

Although the geocell provides greater strength when subjected to inclined shearing force, under heavy vertical load, the shearing force may cause damage to the cell wall, resulting in internal damage to the composite.

Conclusions

When geocells are subjected to lateral earth pressure, the shear strength of the geocell-reinforced soil must be considered. To investigate the interface behavior influenced by



Fig. 6 The gap between boxes during shearing process under 400 kPa normal stress (*RS800**)

cell size, geocell angle to the horizontal plane, and normal stress on the samples in reinforced and unreinforced soil, several large-scale direct shear tests were conducted, and the following conclusions were obtained:

- (1) The geocell significantly enhanced the shear strength of the shear plane. During the shearing process, different geocell angles to the horizontal plane produce different stress–displacement curves. When the angle to the horizontal plane is 0° , the curve is a strain-softening type. When the angle is $45^\circ + \varphi/2$, the curve continues to grow.
- (2) The improvement in strength is mainly reflected in the increased apparent cohesion of the shear plane; an increase in the friction angle has little effect on the shear strength. Small cells can provide greater shear strength, and the reinforcement effect weakens when the normal stress is large, both under maximum and residual shear stress.
- (3) The geocell angle to the horizontal plane greatly affects the characteristics of the shear plane. It can be interpreted that the shear force acts directly on the hybrid shear plane that consists of soil part and geocell part; the total strength is a combination of the geocell and soil resistance to the applied stress.
- (4) This study also investigated the vertical displacement during the shearing process. Contraction was observed at the beginning of the test; as the shear displacement increased, the vertical displacement gradually increased. When the normal stress was smaller, the samples exhibited stronger dilatancy and greater vertical displacement. The main influencing factor is the geocell angle to the horizontal plane; cell size has little effect on the dilatancy of the samples.

Author contribution All authors listed on the manuscript contributed to the study and approved the current version of the manuscript.

Funding This research received support from the special fund for scientific research projects of company SICHUAN Road and Bridge (Group) CO., LTD.

Availability of data and material Data and material in this study are available from the corresponding author upon request.

Code availability There was no code in this article.

Declarations

Conflict of interest The authors declare no competing interests.

References

- Abdumuttalip A, Gizem M (2021) Three-dimensional numerical analysis of geocell reinforced shell foundations. *Geotext Geomembr*. <https://doi.org/10.1016/j.geotextmem.2021.01.006>
- Afzali Nejad A, Lashkari A, Farhadi B (2018) Role of soil inherent anisotropy in peak friction and maximum dilation angles of four sand-geosynthetic interfaces. *Geotext Geomembr* 46(6):869–881. <https://doi.org/10.1016/j.geotextmem.2018.08.003>
- Arvin MR, Abbasi M, Fahlani HK (2021) Shear behavior of geocell-geofabric composite. *Geotext Geomembr* 49(1):188–195. <https://doi.org/10.1016/j.geotextmem.2020.09.012>
- Bathurst R, Karpurapu R (1993) Large-scale triaxial compression testing of geocell-reinforced granular soils. *Geotech Test J* 16(3):296–303. <https://doi.org/10.1520/GTJ10050J>
- Biabani M, Indraratna B, Ngo N (2016) Modelling of geocell-reinforced subballast subjected to cyclic loading. *Geotext Geomembr* 44(4):489–503. <https://doi.org/10.1016/j.geotextmem.2016.02.001>
- Chen RH, Huang YW, Huang FC (2013a) Confinement effect of geocells on sand samples under triaxial compression. *Geotext Geomembr* 37:35–44. <https://doi.org/10.1016/j.geotextmem.2013.01.004>
- Chen RH, Wu CP, Huang FC, Shen CW (2013b) Numerical analysis of geocell-reinforced retaining structures. *Geotext Geomembr* 39:51–62. <https://doi.org/10.1016/j.geotextmem.2013.07.003>
- Dash Sujit K (2010) Influence of relative density of soil on performance of geocell-reinforced sand foundations. *J Mater Civ Eng* 22(5):533–538. [https://doi.org/10.1061/\(ASCE\)MT.1943-5533.0000040](https://doi.org/10.1061/(ASCE)MT.1943-5533.0000040)
- Dash Sujit K (2012) Effect of geocell type on load-carrying mechanisms of geocell-reinforced sand foundations. *Int J Geomech* 12(5):537–548. [https://doi.org/10.1061/\(ASCE\)GM.1943-5622.0000162](https://doi.org/10.1061/(ASCE)GM.1943-5622.0000162)
- Ferreira FB, Vieira CS, Lopes M (2015) Direct shear behaviour of residual soil–geosynthetic interfaces – influence of soil moisture content, soil density and geosynthetic type. *Geosynth Int* 22(3):257–272. <https://doi.org/10.1680/gein.15.00011>
- Hatami K, Esmaili D (2015) Unsaturated soil–woven geotextile interface strength properties from small-scale pullout and interface tests. *Geosynth Int* 22(2):161–172. <https://doi.org/10.1680/gein.15.00002>
- Hegde A (2017) Geocell reinforced foundation beds–past findings, present trends and future prospects: a state-of-the-art review. *Constr Build Mater* 154:658–674. <https://doi.org/10.1016/j.conbuildmat.2017.07.230>

- Hegde A, Sitharam TG (2013) Experimental and numerical studies on footings supported on geocell reinforced sand and clay beds. *Int J Geotech Eng* 7(4):346–354. <https://doi.org/10.1179/1938636213Z.00000000043>
- Khorsandiardebili N, Ghazavi M (2021) Static stability analysis of geocell-reinforced slopes. *Geotext Geomembr* 49(3):852–863. <https://doi.org/10.1016/j.geotextmem.2020.12.012>
- Liu CN, Ho YH, Huang JW (2009) Large scale direct shear tests of soil/PET-yarn geogrid interfaces. *Geotext Geomembr* 27(1):19–30. <https://doi.org/10.1016/j.geotextmem.2008.03.002>
- Lopes ML, Silvano R (2010) Soil/geotextile interface behaviour in direct shear and pullout movements. *Geotech Geol Eng* 28(6):791–804. <https://doi.org/10.1007/s10706-010-9339-z>
- MadhaviLatha G, Somwanshi A (2009) Effect of reinforcement form on the bearing capacity of square footings on sand. *Geotext Geomembr* 27(6):409–422. <https://doi.org/10.1016/j.geotextmem.2009.03.005>
- MoghaddasTafreshi SN, Shaghghi T, Mehrjardi Gh et al (2015) A simplified method for predicting the settlement of circular footings on multi-layered geocell-reinforced non-cohesive soils. *Geotext Geomembr* 43(4):332–344. <https://doi.org/10.1016/j.geotextmem.2015.04.006>
- Neto JOA, Futai MM, Bueno BS (2013) A bearing capacity calculation method for soil reinforced with a geocell. *Geosynth Int* 20(3):129–142. <https://doi.org/10.1680/gein.13.00007>
- Rajagopal K, Krishnaswamy NR, Latha GM (1999) Behaviour of sand confined with single and multiple geocells. *Geotext Geomembr* 17(3):171–184. [https://doi.org/10.1016/S0266-1144\(98\)00034-X](https://doi.org/10.1016/S0266-1144(98)00034-X)
- Research Institute of Highway Ministry of Transport (2006) Test methods of geosynthetics for highway engineering (JTG E50–2006). Shanghai
- Simoni A, Houlsby GT (2006) The direct shear strength and dilatancy of sand–gravel mixtures. *Geotech Geol Eng* 24(3):523. <https://doi.org/10.1007/s10706-004-5832-6>
- Song F, Liu HB, Ma LQ, Hu HB (2018) Numerical analysis of geocell-reinforced retaining wall failure modes. *Geotext Geomembr* 46(3):284–296. <https://doi.org/10.1016/j.geotextmem.2018.01.004>
- TavakoliMehrjardi G, Motarjemi F (2018) Interfacial properties of geocell-reinforced granular soils. *Geotext Geomembr* 46(4):384–395. <https://doi.org/10.1016/j.geotextmem.2018.03.002>
- TavakoliMehrjardi G, Behrad R, MoghaddasTafreshi SN (2019) Scale effect on the behavior of geocell-reinforced soil. *Geotext Geomembr* 47(2):154–163. <https://doi.org/10.1016/j.geotextmem.2018.12.003>
- Thallak SG, Saride S, Dash SK (2007) Performance of surface footing on geocell-reinforced soft clay beds. *Geotech Geol Eng* 25(5):509. <https://doi.org/10.1007/s10706-007-9125-8>
- Wang YM, Chen YK, Liu W (2008) Large-scale direct shear testing of geocell reinforced soil. *J Cent South Univ Technol* 15(6):895–900. <https://doi.org/10.1007/s11771-008-0163-z>
- Yang X (2005) Study on engineering character and applied technique of geocell. Chang'an University
- Zhang MX, Javadi AA, Min X (2006) Triaxial tests of sand reinforced with 3D inclusions. *Geotext Geomembr* 24:201–209. <https://doi.org/10.1016/j.geotextmem.2006.03.004>
- Zhou HB, Wen XJ (2008) Model studies on geogrid- or geocell-reinforced sand cushion on soft soil. *Geotext Geomembr* 26(3):231–238. <https://doi.org/10.1016/j.geotextmem.2007.10.002>